Tracking the catalyzed growth process of nanowires by *in situ* x-ray diffraction

Melanie Kirkham, Zhong Lin Wang, and Robert L. Snyder[a)]
School of Materials Science and Engineering, Georgia Institute of Technology, Atlanta, Georgia 30332-0245, USA

(Received 24 December 2009; accepted 17 May 2010; published online 6 July 2010)

Quasi-one-dimensional nanostructures of silicon, oxides, and other materials show great promise for a variety of applications. These nanostructures are commonly grown using metal catalyst nanoparticles. This paper investigates the growth mechanism of Au-catalyzed Si nanowires through *in situ* x-ray diffraction, and the results are compared to previously studied Au-catalyzed ZnO nanorods. The Si nanowires were found to grow from molten catalyst particles, however, the ZnO nanorods were found to grow from solid catalyst particles through a surface diffusion process. From this comparison, the relative bonding types of the catalyst and source material are determined to have a significant effect on the growth mechanism. © *2010 American Institute of Physics*. [doi:10.1063/1.3452342]

I. INTRODUCTION

Silicon nanowires have been the subject of much research, due to their potential applications in many different areas. They have been demonstrated for use in electrical sensing in biosystems.[1–3] Silicon nanowires perform better than traditional materials in anodes for lithium ion batteries, having a higher charge capacity.[4–7] Silicon nanowires have also found application in solar cells, both as absorber and as an antireflective coating.[8–11] Basic logic and memory elements including silicon nanowires have been demonstrated,[12,13] presaging applications in nanoelectronics.

Silicon nanowires are commonly grown by bottom-up approaches involving the deposition of a Si-containing vapor source material on the surface of a metal catalyst. From investigations of Au-catalyzed Si whiskers (i.e., high aspect ratio crystals in the micron range), Wagner and Ellis formulated in 1964 the vapor-liquid-solid (VLS) growth mechanism.[14,15] In the VLS mechanism, the source material, supplied in vapor form, is decomposed on the surface of and absorbed into the catalyst particle. The catalyst particle melts to the liquid state due to a eutectic reaction with the source material. Source material continues to dissolve into the liquid catalyst particle until it becomes supersaturated, at which point a solid particle nucleates on the surface. Continued growth at the interface between the liquid catalyst and solid particle leads to the formation of a one-dimensional (1D) nanostructure. The VLS mechanism was generally accepted for the growth of whiskers and later applied to the catalyzed growth of 1D nanostructures of silicon and other materials, including compound semiconductors and oxides. However, the growth mechanism is still not fully understood, with questions remaining about the state of the catalyst particle during growth[16,17] and the diffusion path of the source material to the growth front.[18–20]

The purpose of this research is to investigate the growth mechanism of catalyzed 1D nanostructures through *in-situ* x-ray diffraction analysis during the growth of Au-catalyzed Si nanowires. Information concerning the catalyst particle state during growth and the diffusion path of the growth species to the growth front is obtained and compared to our previously published results for Au-catalyzed ZnO nanorods.[21] From this comparison, the relative bonding types of the catalyst and source material are determined to have a significant effect on the growth mechanism.

II. SYNTHESIS AND CHARACTERIZATION OF NANOSTRUCTURES

Gold-catalyzed silicon nanowires were grown in an x-ray furnace so that *in situ* x-ray diffraction data could be collected during growth. The nanowires were grown in an Anton-Paar HTK1200 oven-type furnace attached to a Panalytical X'Pert PRO diffractometer. The temperature of the furnace was validated using known phase transitions of standard materials. The substrates, surface oxidized single-crystal Si (100) sputtered with 5 to 10 nm of gold, were placed in the center of the furnace. Prior to heating, the furnace was evacuated to a base pressure around 10^{-3} to 10^{-2} mbar. The residual oxygen was further reduced by purging the chamber with N_2 and by holding the furnace at the growth temperature for 1 h prior to starting growth. The growth temperature was 685 °C. The source gas, a mixture of 1% silane (SiH_4) in nitrogen was flowed for 30–60 min. The growth pressure was around 3 mbar, and after growth the furnace was cooled under vacuum (around 10^{-3} mbar).

The samples were imaged with scanning electron microscopy as shown in Figs. 1(a) and 1(b). The density of nanowire growth is high, with the nanowires forming a tangled layer. Measuring the nanowire lengths is difficult, due to the tangled nature of the growth. However, the lengths appear to be on the order of several microns or greater. The nanowires have diameters of 21 ± 7 nm. The aspect ratio of the nanowires is on the order of 100.

Closer examination with transmission electron microscopy (TEM) reveals catalyst particles at the tips of the nano-

a)Electronic mail: robert.snyder@mse.gatech.edu

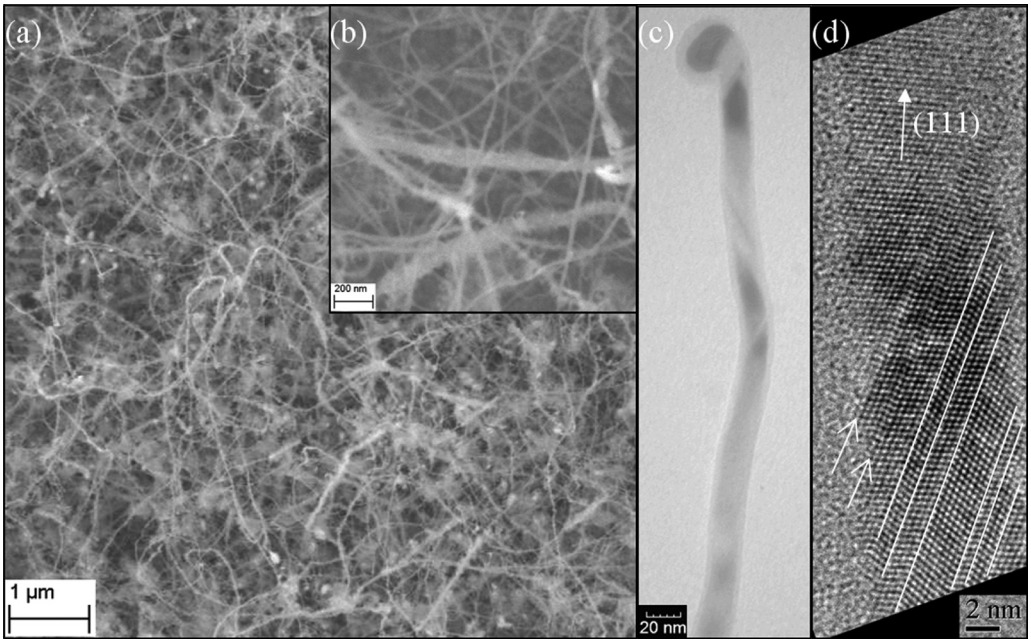

FIG. 1. Au-catalyzed Si nanowires grown via silane decomposition, imaged with (a) and (b) scanning electron microscopy (SEM), (c) TEM, showing catalyst particle and amorphous layer, and (d) HRTEM, showing (111) growth direction, (111) twin planes (lines) and stacking faults (arrows).

wires, as seen in Fig. 1(c). The catalyst particles are roughly hemispherical in shape, with diameters around 20 nm. The catalyst particles and nanowires are covered with a layer, around 2 nm thick, which is likely amorphous silica. Energy dispersive spectroscopy (EDS) spectra from areas including and not including catalyst particles confirm the presence of Au in the catalyst particles, and its absence in the nanowires, as seen in Fig. 2. The Cu and C peaks are from the TEM grid and film. The O peak may come from impurities in the carbon grid or from amorphous silica.

In order to further investigate the synthesis process, several control samples were made, keeping the same conditions, but changing one key factor in each control. For one sample, no gold was deposited on the substrate. Without the gold, no nanowires grew, though some rough deposition, presumably silicon, was observed on the substrate indicating that gold is necessary to catalyze the growth of nanowires. For another control sample, the substrates were coated with gold, but the N_2/silane mixture source gas was replaced with pure N_2 gas. Again, no nanowires grew, indicating that the silane is necessary for growth, and suggesting that the silicon substrate does not contribute to the process.

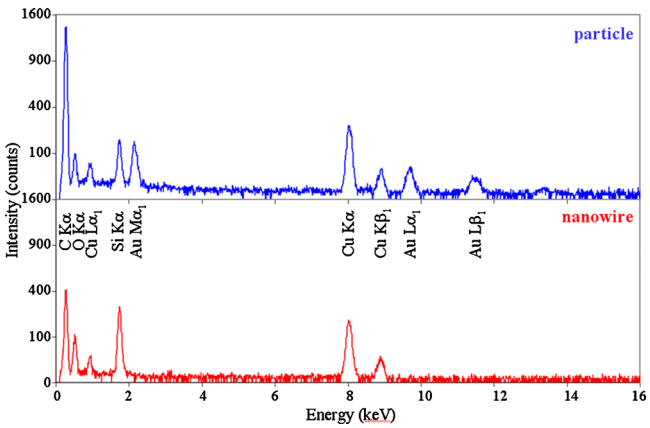

FIG. 2. (Color online) EDS spectra collected in TEM from an area containing a catalyst particle (top) and an area containing only a nanowire (bottom).

The nanowires were further characterized with high-resolution transmission electron microscopy (HRTEM), as seen in Fig. 1(d). The nanowires are crystalline, with a growth direction of [111], determined from the average lattice spacing of around 3.5 Å, which is consistent with the expected (111) lattice spacing. HRTEM images collected from some curved areas of the nanowires show crystal defects, namely (111) twins and stacking faults. The observed crystal defects may allow the nanowires to remain crystalline while they are strongly curved.

III. *IN SITU* X-RAY ANALYSIS

In situ x-ray diffraction (XRD) data were collected during the growth of the silicon nanowires with Cu $K\alpha_1$ radiation. An incident-side Göbel mirror and a linear position sensitive detector were used for fast data collection. This x-ray optic combination is susceptible to peak shift due to sample surface displacement, therefore usable information is derived based on peak intensity only, not position. The *in situ* XRD data for a typical sample are shown in Fig. 3. In the initial heating stage, the gold (111) peak increases in intensity and narrows. This is indicative of the as-sputtered gold increasing in crystallite size as it is annealed, and forming (111)-oriented nanoparticles. During the 1 h hold at the growth temperature before the introduction of silane, there is little change in the x-ray scans. Once the silane flow starts, the gold peaks immediately and quickly begin to disappear, indicating that the gold nanoparticles are losing their crystal structure. The gold peaks reappear after cooling to room temperature, as the gold resolidifies from the molten state. After

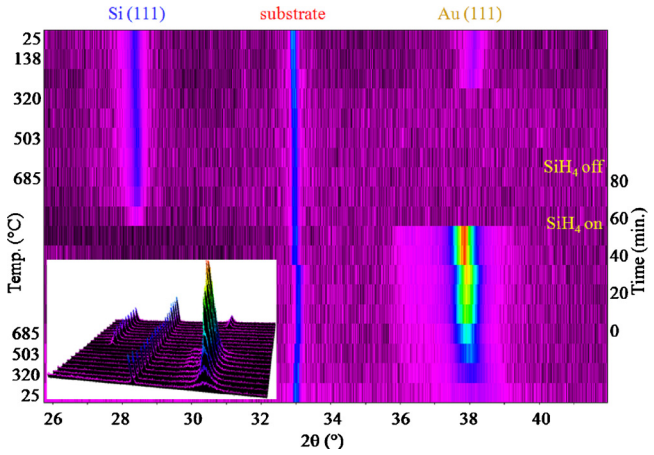

FIG. 3. (Color online) *In situ* XRD data from the growth of Au-catalyzed Si nanowires. Each horizontal line is one XRD scan, with the intensity represented by the color. The first scan is at the bottom, and time progresses upward. The inset shows the same data in a three-dimensional view.

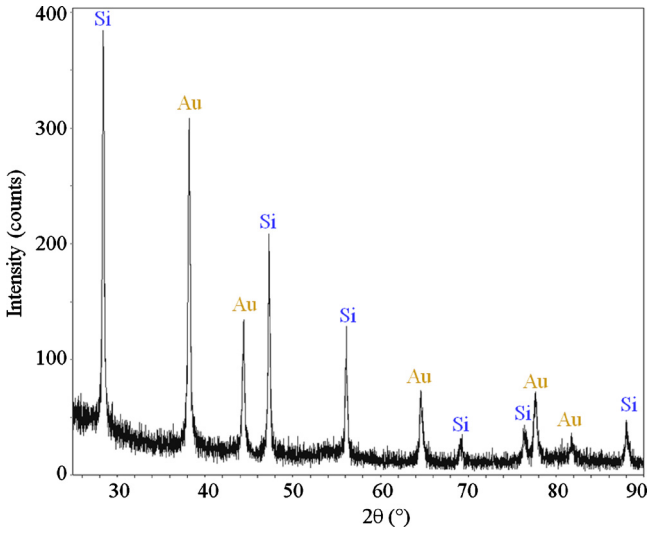

FIG. 4. (Color online) GIXRD scan of Au-catalyzed Si nanowires.

growth, the gold signal is that of a randomly oriented polycrystalline material. As the gold is now at the tips of the nanowires, it no longer preserves an epitaxial relationship with the substrate. For samples where nanowires did not grow, the gold did not melt, with only one outlier.

For several samples, *in situ* XRD data were also collected during cooling after growth, in order to investigate the gold recrystallization temperature. The gold peaks do not reappear until the scan collected at 284 °C. This is significantly below the gold–silicon eutectic temperature of ~364 °C.[22] The eutectic temperature may be lowered for the Au nanoparticles due to the Gibbs–Thompson effect, as has been previously reported during the growth of Ge nanowires.[23] The Gibbs–Thompson effect relates the radius of curvature of a particle, and consequently the diameter, to the vapor pressure and further to other properties, including the melting temperature.

IV. POSTGROWTH X-RAY DIFFRACTION CHARACTERIZATION

After synthesis in the x-ray furnace, the silicon nanowire samples were further characterized using additional x-ray diffraction techniques. The additional XRD data collection was optimized for accurate lattice parameter determination, with a Göbel mirror, 0.09° parallel plate collimator, and 0.04 rad Soller slits. The radiation was Cu $K\alpha_1$. Since the nanowires are not preferentially aligned, as can be clearly seen in the SEM images, the grazing incidence technique could be employed to increase the signal from the nanowires. Additionally, as the substrate is single crystal, diffraction peaks due to the substrate will not appear in grazing incidence x-ray diffraction (GIXRD) scans, allowing the signal from the nanowires to be clearly distinguished. Signals from both the gold catalyst particles and silicon nanowires are present, as seen in Fig. 4. No other phases are observed.

Since many peaks from each phase may be observed, Pawley whole pattern fitting may be applied to the scans. For this sample, the patterns were fit using a second-order polynomial background curve and a pseudo-Voigt peak shape function. Two-theta zero and sample surface displacement errors were not refined, as they were minimized by aligning the instrument before measurement and through the use of parallel beam optics, respectively. At least three GIXRD scans were collected from each of three samples, and the results averaged.

For the gold phase in post thermally processed samples, the lattice parameter averaged over three samples was determined to be 4.0731 ± 0.0025 Å. This value is statistically the same (i.e., within 3σ) as that measured from a control sample never exposed to SiH_4 (4.0785 ± 0.0006 Å), which indicates that there is no significant amount of Si dissolved into the Au. Alloying of Si into Au should cause a significant decrease in the gold lattice parameter.[24,25] As no significant decrease was seen in the gold lattice parameter from samples with Si nanowires, it may be concluded that there is no Si in the Au after growth.

The melting point of pure gold (1063 °C) is well above the growth temperature of the nanowires, even when accounting for the Gibbs–Thompson effect on the melting point of nanosized particles.[26] Therefore, silicon must have dissolved into the gold catalyst particles during growth, in order to cause eutectic melting. (The Au–Si eutectic temperature, 366 °C, is below the growth temperature.[22]) However, as shown above, no silicon is present in the gold at room temperature after growth. From the phase diagram,[22] it may be seen that there is little solid solubility of silicon in gold. This is supported by literature reports, which have found that rapid quenching from a Au–Si melt is necessary to prevent the formation of separate gold and silicon phases upon solidification.[27,28] Therefore, the silicon likely exsolves out of the gold nanoparticles as the gold nanoparticles recrystallize on cooling. The small dimensions of the nanoparticles may allow the silicon time to diffuse to the surface, where it forms a thin shell, as seen in Fig. 1(c).

V. IMPLICATIONS FOR THE GROWTH MODEL

In the VLS mechanism, the catalyst particle is liquid during growth. However, some studies in the literature have

reported that 1D nanostructures may also be grown by solid catalyst particles, which has been termed the vapor-solid-solid mechanism. In an early study of Ti-catalyzed Si nanowires were grown from silane at temperatures around 700° below the eutectic temperature (around 1330 °C).[29] Since then, there have been more reports of 1D nanostructure growth from solid catalyst particles, in most cases for growth below the eutectic temperature. Kodambaka *et al.*[30] investigated nanowire growth *in situ* in a TEM. They found that nanowires could grow from solid and liquid catalysts at the same temperature, depending on the source material pressure and thermal history. Some studies of Au-catalyzed InAs and InP nanowires have even reported that growth could only occur with solid catalyst particles,[31,32] as no nanowire growth was observed above the eutectic temperature.

The above results on gold-catalyzed silicon nanowires have some interesting implications for the growth model. The *in situ* XRD data clearly and conclusively show that the gold catalyst particles are molten during nanowire growth. This is in contrast to our previously published results for gold-catalyzed ZnO nanowires,[21] where the catalyst particle was determined to be solid during growth. Although the growth temperatures were above the Au–Zn eutectic temperature, no Zn was present in the gold to cause eutectic melting. The presence of a solid catalyst particle was verified with high-temperature XRD data collected postgrowth.

In the conventional understanding of the VLS mechanism, diffusion of the source material to the growth front occurs through the catalyst particle (bulk). However, a few studies have pointed to the possibility of surface diffusion around the catalyst particle.[33,34] Experimental evidence for surface diffusion was found in a study of the growth of Ni, Co, and Fe catalyzed carbon nanofibers.[20] The authors measured a low activation energy, comparable to that for the diffusion of carbon on Ni and Co surfaces and much smaller than for the diffusion of carbon through bulk Ni and Co. Also, a study of Au-catalyzed InAs/GaAs heterostructures found a sharp interface between InAs and GaAs when the source material was switched during growth from trimethyl indium to triethyl gallium.[35] If growth proceeds by bulk supersaturation, a region of mixed composition should have been observed.

The high surface-to-volume ratio in the nanosize regime causes surface related effects to gain prominence, and surface diffusion coefficients are generally several orders of magnitude larger than bulk diffusion coefficients, due to broken and dangling bonds on the surface. Therefore, it is reasonable that the catalyzed growth of 1D nanostructures could proceed by surface diffusion of the growth species around the catalyst. In addition, metal nanoparticles will have a quasiliquid layer (QLL) on the surface.[36,37] The high surface curvature of nanoparticles causes the surface atoms to adopt a disordered arrangement in order to reduce the surface energy, with a liquidlike structure,[38] which would have a high sticking coefficient for preferential adsorption. QLLs have been found to have unusually high diffusion coefficients, to the point of approaching, or even exceeding, the bulk liquid diffusion coefficient at temperatures approaching the melting point.[39] The presence of such a liquidlike layer on the surface of the catalyst particles would further favor surface diffusion of the growth species to the growth front.

For the Au-catalyzed Si nanowires, the diffusion path was determined to be through the bulk of the catalyst, as the dissolution of Si into the Au is necessary for the observed eutectic melting. However, for Au-catalyzed ZnO nanowires, the diffusion path was determined to be along the surface of the catalyst, as the gold lattice parameters indicated that no Zn was dissolved in the gold, as previously reported.[21]

Both the question of the catalyst particle state (at temperatures between the eutectic and bulk melting temperatures) and the source material diffusion path fundamentally come down to whether or not the source material will diffuse into the catalyst particle. From our previous research, it was found that in the case of Au-catalyzed ZnO nanostructures, the growth species did not diffuse into the catalyst particle, resulting in solid catalyst particles during growth and a surface diffusion path of the source material.[21] From the current research on Au-catalyzed Si nanostructures, it was found that the growth species did diffuse into the catalyst particle, resulting in liquid catalyst particles during growth and a largely bulk diffusion path of the source material.

By comparing the results, it may be observed that in the case where the growth species did not diffuse into the catalyst particle, the source material was ionic, and in the case where the growth species did diffuse into the catalyst particle, the source material was nonionic. This difference in bonding type of the source material may explain the difference in the results. As in the general chemical principle of "like dissolves like," chemical species will more likely dissolve in a solvent of the same bonding type. Since the catalyst particle in all cases was metallic, the ionic growth species (for ZnO) would be unlikely to dissolve into the catalyst particle. However, the nonionic growth species (for Si) would be more likely to dissolve into the catalyst particle, allowing a bulk diffusion path and causing eutectic melting of the catalyst particle. In this way, the catalyst particle state and diffusion path are connected, and the same relationships that favor solid catalyst particles also favor a surface diffusion path.

VI. CONCLUSIONS

In situ XRD data were collected during the growth of Au-catalyzed Si nanowires. The gold catalyst particles were directly observed to be molten during growth. At the growth temperature, melting of the gold requires a eutectic interaction, implying the bulk diffusion of Si into the Au. These findings for Au-catalyzed Si nanowires are consistent with the conventional understanding of the VLS mechanism. However, our previously published results on Au-catalyzed ZnO nanorods[21] found solid catalyst particles during growth and surface diffusion of the source material to the growth front.

The difference between the gold catalyst behavior for Si or ZnO nanostructures points toward the importance of the source material bonding type. In cases with compatible bond types between the source material and catalyst, as in the Au-catalyzed Si nanowires, the source material may diffuse

into the catalyst particle and result in eutectic lowering of the melting temperature. In cases with incompatible bond types, as in the Au-ZnO nanorods, the source material cannot diffuse into the catalyst particle to cause eutectic lowering of the melting temperature.

These findings have important implications toward the synthesis of 1D nanostructures for technologically important applications. A better understanding of the synthesis mechanism allows better control. Knowledge of the importance of the source material and catalyst bonding type allows for an informed choice of appropriate source materials and catalysts. The ability to grow 1D nanostructures with solid catalysts opens up the possibility of low temperature growth on polymer substrates, for flexible devices. These findings can aid the utilization of 1D nanostructures for second generation, active nanotechnology applications, in chemical sensing, optical, photovoltaic, energy generation, and other areas.

ACKNOWLEDGMENTS

The authors would like to thank Dr. Yong Ding for his help with HRTEM measurements.

[1]S. Roy and Z. Gao, Nanotoday **4**, 318 (2009).
[2]F. Patolsky, B. P. Timko, G. Yu, Y. Fang, A. B. Greytak, G. Zheng, and C. M. Lieber, Science **313**, 1100 (2006).
[3]B. P. Timko, T. Cohen-Karni, G. Yu, Q. Qing, B. Tian, and C. M. Lieber, Nano Lett. **9**, 914 (2009).
[4]C. K. Chan, H. Peng, G. Liu, K. McIlwrath, X. F. Zhang, R. A. Huggins, and Y. Cui, Nat. Nanotechnol. **3**, 31 (2008).
[5]C. K. Chan, R. Ruffo, S. S. Hong, R. A. Huggins, and Y. Cui, J. Power Sources **189**, 34 (2009).
[6]K. Peng, J. Jie, W. Zhang, and S.-T. Lee, Appl. Phys. Lett. **93**, 033105 (2008).
[7]R. Ruffo, S. S. Hong, C. K. Chan, R. A. Huggins, and Y. Cui, J. Phys. Chem. C **113**, 11390 (2009).
[8]H. Fang, X. Li, S. Song, Y. Xu, and J. Zhu, Nanotechnology **19**, 255703 (2008).
[9]K. Peng, X. Wang, and S.-T. Lee, Appl. Phys. Lett. **92**, 163103 (2008).
[10]T. Stelzner, M. Pietsch, G. Andrä, F. Falk, E. Ose, and S. Christiansen, Nanotechnology **19**, 295203 (2008).
[11]L. Tsakalakos, J. Balch, J. Fronheiser, B. A. Korevaar, O. Sulima, and J. Rand, Appl. Phys. Lett. **91**, 233117 (2007).
[12]Y. Huang, X. Duan, Y. Cui, L. J. Lauhon, K.-H. Kim, and C. M. Lieber, Science **294**, 1313 (2001).
[13]X. Duan, Y. Huang, and C. M. Lieber, Nano Lett. **2**, 487 (2002).
[14]R. S. Wagner and W. C. Ellis, Appl. Phys. Lett. **4**, 89 (1964).
[15]R. S. Wagner and W. C. Ellis, Trans. Metall. Soc. AIME **233**, 1053 (1965).
[16]K. Busuttil, Mater. Today **10**, 18 (2007).
[17]V. Schmidt and U. Gösele, Science **316**, 698 (2007).
[18]A. I. Persson, L. E. Fröberg, S. Jeppesen, M. T. Björk, and L. Samuelson, J. Appl. Phys. **101**, 034313 (2007).
[19]L. E. Jensen, M. T. Björk, S. Jeppesen, A. I. Persson, B. J. Ohlsson, and L. Samuelson, Nano Lett. **4**, 1961 (2004).
[20]S. Hofmann, G. Csnyi, A. C. Ferrari, M. C. Payne, and J. Robertson, Phys. Rev. Lett. **95**, 036101 (2005).
[21]M. Kirkham, X. Wang, Z. L. Wang, and R. L. Snyder, Nanotechnology **18**, 365304 (2007).
[22]F. G. Meng, H. S. Liu, L. B. Liu, and Z. P. Jin, J. Alloys Compd. **431**, 292 (2007).
[23]H. Adhikari, A. F. Marshall, C. E. D. Chidsey, and P. C. McIntyre, Nano Lett. **6**, 318 (2006).
[24]H. L. Luo, W. Klement, Jr., and T. R. Anantharaman, Trans. Indian Inst. Met. **18**, 214 (1965).
[25]W. Robison, R. Sharma, and L. Eyring, Acta Metall. Mater. **39**, 179 (1991).
[26]P. Buffat and J. P. Borel, Phys. Rev. A **13**, 2287 (1976).
[27]C. Suryanarayana and T. R. Anantharaman, Mater. Sci. Eng. **13**, 73 (1974).
[28]D. K. George, A. A. Johnson, and R. J. Storey, Mater. Sci. Eng., B **55**, 221 (1998).
[29]T. I. Kamins, R. S. Williams, D. P. Basile, T. Hesjedal, and J. S. Harris, J. Appl. Phys. **89**, 1008 (2001).
[30]S. Kodambaka, J. Tersoff, M. C. Reuter, and F. M. Ross, Science **316**, 729 (2007).
[31]K. A. Dick, K. Deppert, T. Mårtensson, B. Mandl, L. Samuelson, and W. Seifert, Nano Lett. **5**, 761 (2005).
[32]J. Johansson, B. A. Wacaser, K. A. Dick, and W. Seifert, Nanotechnology **17**, S355 (2006).
[33]H. Wang and G. S. Fischman, J. Appl. Phys. **76**, 1557 (1994).
[34]P. Cheyssac, M. Sacilotti, and G. Patriarche, J. Appl. Phys. **100**, 044315 (2006).
[35]B. J. Ohlsson, M. T. Björk, A. I. Persson, C. Thelander, L. R. Wallenberg, M. H. Magnusson, K. Deppert, and L. Samuelson, Physica E (Amsterdam) **13**, 1126 (2002).
[36]W. Krakow, M. Jóse-Yacamán, and J. L. Aragón, Phys. Rev. B **49**, 10591 (1994).
[37]P. M. Ajayan and T. J. Marks, Phys. Rev. Lett. **63**, 279 (1989).
[38]Z. L. Wang, J. M. Petroski, T. C. Green, and M. A. El-Sayed, J. Phys. Chem. B **102**, 6145 (1998).
[39]J. W. M. Frenken, J. P. Toennies, and C. Wöll, Phys. Rev. Lett. **60**, 1727 (1988).